

# Journal Pre-proof

Controlled patterning of upconversion nanocrystals through capillary force

Yiming Wu, Jiahui Xu, Xiaogang Liu



PII: S1002-0721(19)30979-2

DOI: <https://doi.org/10.1016/j.jre.2020.01.015>

Reference: JRE 695

To appear in: *Journal of Rare Earths*

Received Date: 6 December 2019

Revised Date: 16 January 2020

Accepted Date: 17 January 2020

Please cite this article as: Wu Y, Xu J, Liu X, Controlled patterning of upconversion nanocrystals through capillary force, *Journal of Rare Earths*, <https://doi.org/10.1016/j.jre.2020.01.015>.

This is a PDF file of an article that has undergone enhancements after acceptance, such as the addition of a cover page and metadata, and formatting for readability, but it is not yet the definitive version of record. This version will undergo additional copyediting, typesetting and review before it is published in its final form, but we are providing this version to give early visibility of the article. Please note that, during the production process, errors may be discovered which could affect the content, and all legal disclaimers that apply to the journal pertain.

© 2020 Chinese Society of Rare Earths. Published by Elsevier B.V. All rights reserved.

## Controlled patterning of upconversion nanocrystals through capillary force

Yiming Wu<sup>1</sup>, Jiahui Xu<sup>1</sup>, Xiaogang Liu<sup>1,2\*</sup>

<sup>1</sup>*Department of Chemistry, National University of Singapore, 117543, Singapore*

<sup>2</sup>*The N.1 Institute for Health, National University of Singapore, Singapore, 117456, Singapore.*

\*Correspondence to [chmlx@nus.edu.sg](mailto:chmlx@nus.edu.sg)

**Keywords:** upconversion nanoparticles, self-assembly, patterning, rare earths

**ABSTRACT:** Lanthanide-doped upconversion nanoparticles (UCNPs) can absorb near-infrared photons and convert them into visible and ultraviolet emissions. These nanomaterials possess extraordinary optical performance and hold potential as active platforms for a variety of technological applications. The ability to fabricate highly ordered nanoparticle-based photonic elements over a large area is of fundamental significance for luminescence tuning. Despite all the efforts made, however, large-area spatial patterning of UCNPs into ordered arrays with high controllability remains a challenge. In this study, we report a high-throughput strategy to pattern optical nanomaterials through the use of polymer microspheres and templated assembly of UCNPs. This technique utilizes capillary force to drive hybrid clusters into the physical template, resulting in large-area, spatially ordered arrays of particles. The findings reported in this work may promote the development of novel nonlinear optical devices, such as solid-state laser arrays, high-density optical storage, and anti-counterfeiting labels.

## 1. Introduction

Site-specific positioning of nanoparticles onto a large-area substrate with high precision is crucial to harness the collective properties of nanoparticle assemblies for nanophotonic and nanoelectronic applications [1-3]. Lanthanide-doped UCNPs have drawn considerable attention over the past few years because of their fundamental optical properties and technical potentials [4-6]. Owing to their sharp emission band, massive anti-stokes shift, and excellent photosensitivity as well as spectral tunability, UCNPs have found a wide range of applications, including solid-state lasing, security marking, three-dimensional display, optical storage and photovoltaics [7-18]. Assembling UCNPs into highly ordered nanostructures with precisely controlled composition, morphology and optical property makes possible the exploration of new properties and construction of miniaturized photonic devices. For example, the positioning of UCNPs at single-particle levels enables potential application in high-density optical data storage in which bit-patterned media depends on the ability to address single nanoparticles optically [19, 20]. In another case, programmable assembly of different types of UCNPs with distinct color emission and decay dynamics into an ordered array allows new anti-counterfeiting technologies to be developed with high levels of security [21, 22].

Thus far, a variety of techniques have been used to pattern UCNPs for diverse applications. For example, Chen et al. reported the selective assembly of UCNPs onto hydrophobic patterns on surface-modified substrates [23]. Alternatively, the effect of electrostatic interaction has also been harnessed to immobilize different types of UCNPs on a surface at predefined positions [24]. In another study, Ressier's group constructed anti-counterfeiting microtags by utilizing a nanosized tip to create negatively charged patterns for selective assembly of oppositely charged UCNPs [25]. Micro-molding in capillaries was also successfully deployed to make nanoparticle arrays [26, 27]. Inkjet-printing is another attractive method for direct-writing of UCNP micropatterns with conceived security features [28]. Both epitaxial end-on growth and flow lithography techniques have proven effective in producing complex micrometer-sized multicolor barcodes for anti-counterfeiting applications [10, 29]. Despite the enormous efforts, spatial patterning of UCNP assemblies with high precision remains a difficult task.

Herein, we report a general and highly efficient strategy to achieve controlled assembly of UCNPs onto patterned surfaces over a large area. A layer-by-layer assembly technique was used to immobilize nanoparticles onto polymer microspheres. Nanoparticle-modified polymer microspheres serve as the building block for subsequent templated self-assembly. Our experimental results suggest that capillary force plays a crucial role in driving UCNP-modified microspheres onto the template. The strategy reported in this work provides a robust tool to build patterned hierarchical arrays of UCNPs with tunable optical properties and surface functions.

## 2. Experimental

### 2.1. Materials and characteristics

Ytterbium(III) acetate hydrate (99.9%), yttrium(III) acetate hydrate (99.9%), erbium(III) acetate hydrate (99.9%), oleic acid (90%), 1-octadecene (90%), sodium hydroxide (NaOH; >98%), ammonium fluoride (NH<sub>4</sub>F; >98%) and cyclohexane were purchased from Sigma-Aldrich and used as received.

Transmission electron microscopy (TEM) imaging was recorded from a JEOL-JEM 2100F electron microscope. Scanning electron microscopy (SEM) images were taken on a JEOL-JSM-6701F electron microscope. The optical characterization was carried out using the custom-built microscope coupled with a 980 nm continuous-wave excitation laser, capable of wide-field imaging and spectroscopy.

### 2.2. Synthesis of the NaLnF<sub>4</sub> nanocrystals

NaYF<sub>4</sub>:Yb/Er (5 mol%/2 mol%) nanocrystals were prepared according to previous reports [30, 31]. Typically, to a 50-mL flask containing 3 mL of oleic acid, 1.86 mL of Y(CH<sub>3</sub>CO<sub>2</sub>)<sub>3</sub>, 100 μL of Yb(CH<sub>3</sub>CO<sub>2</sub>)<sub>3</sub> and 40 μL of Er(CH<sub>3</sub>CO<sub>2</sub>)<sub>3</sub> were added. The reaction mixture was heated at 150 °C for 30 min under stirring to remove the water residue. Then, 7 mL of 1-octadecene were then quickly introduced into the reaction mixture, followed by heating at 150 °C for another 30 min before cooling to 50 °C. Shortly after that, 1.6 mmol NH<sub>4</sub>F and 1 mmol NaOH methanol solution were added to the reaction mixture under stirring for another 30 min. After evaporation of the methanol, the solution was heated at 290 °C under argon for 1.5 h

and then cooled to room temperature. The resulting nanoparticles were precipitated by addition of ethanol, collected by centrifugation, washed with ethanol twice, and re-dispersed in 4 mL of cyclohexane. The synthesis procedure of NaYF<sub>4</sub>:Yb/Tm (30 mol %/0.5 mol%) nanoparticles and NaYF<sub>4</sub>:Yb/Er (60 mol %/2 mol %) nanocrystals are similar to that presented above.

### **2.3. Preparation of hydrophilic ligand-free NaLnF<sub>4</sub> nanoparticles**

The as-prepared oleic acid-capped nanoparticles were dispersed in a 2-mL HCl solution (0.1 mol/L) and ultrasonicated for 10 min to remove surface ligands. After the reaction, the nanoparticles were collected via centrifugation and further purified by adding an acidic ethanol solution. The resulting products were washed with ethanol and deionized water several times, and re-dispersed in 4 mL of deionized water.

### **2.4. Preparation of UCNP-coupled polystyrene (PS) colloidal beads**

Positively charged poly(diallyldimethylammonium chloride) and negatively charged poly(sodium 4-styrenesulfonate) were used as polyelectrolytes. Aqueous dispersions of PS spheres with a diameter of 2 μm were purchased from Sigma-Aldrich. The dispersion concentration was adjusted to the value of 1% of solid content by dilution with deionized water. Typically, 5 μL of the PS bead solution was added into 0.5 mL of 10 mmol/L poly(diallyldimethylammonium chloride) solution containing 0.5 mol/L sodium chloride. After incubation for 30 min, PS beads were centrifugated at 3000 r/min for 3 min and then washed with DI water three times. Positively charged PS spheres were added into 0.5 mL of 10 mmol/L poly(sodium 4-styrenesulfonate) solution containing 0.5 r/min sodium chloride and kept in solution for 30 min, followed by three cycles of centrifugation, washing and redispersion in 0.2 mL water. For coating of UCNPs, 50 μL of 0.1 mol/L nanoparticle solution was added into the as-prepared polyelectrolyte treated PS bead solution. This mixture was placed on a shaker for 1 h, followed by being cleaned three times by centrifugation and washing. Finally, the UCNPs coated PS microspheres were re-dispersed in an aqueous solution containing 0.25% sodium dodecyl sulfate.

### **2.5. Fabrication of fluidic cells**

The photoresist pattern arrays were fabricated on ITO glass substrates by UV photolithography. In a typical procedure, the bottom of the ITO substrate was cleaned with

acetone and ethanol, ultrasonicated for 10 min, and then treated with UV (ultraviolet) rays-ozone for 15 min. A uniform thin film of positive photoresist (AZ1518) was spin-coated at 3000 rpm for 60s onto the substrate, and soft-baked at 90 °C for 2 min and then selectively exposed to UV rays. After development and washing with water, the photoresist patterned arrays were formed on ITO surface. The experimental setup consists of two parallel pieces of ITO glass separated by a thick double-sided tape (100 μm). The UCNP-tethered PS colloidal particles were dispersed in deionized water containing 0.25% sodium dodecyl sulfate and then injected into the cell. Digital imaging mounted on an optical microscope was used to monitor the assembly process.

### 3. Results and discussion

For upconversion nanomaterials, near-infrared photons are absorbed by sensitizer ions (e.g., trivalent yttrium ions) and subsequently transferred to nearby activator ions capable of generating diverse color emissions from a high energy level (Fig. 1(a-c)). We began with the synthesis of three types of NaLnF<sub>4</sub> UCNPs with three primary colors (red, green and blue), as shown in Figure 1d. In principle, mixing three types of NaLnF<sub>4</sub> UCNPs at different proportions can produce a full range of colors spanning almost the entire visible spectrum. The key to successful site-specific patterning of UCNPs is to synthesize a stable dispersion of spherical UCNP-coupled PS beads for templated self-assembly. PS spheres with controllable size and low density are easily to form the aqueous colloidal suspension. To this end, we investigated several potential routes to coat PS beads with UCNPs. We first considered the solvent swelling method, based on the swelling of PS beads and the diffusion of UCNPs. However, we found that the resulting PS beads exhibit strong surface textures and tend to aggregate into nonuniform clusters (Fig. 2(a)). This treatment leads to poor dispersibility, unsuitable for patterning ordered microbead arrays.

A straightforward method than utilizing in-situ dispersion polymerization of UCNPs into polymer beads was also investigated in this work. The synthesis of UCNP-coupled PS beads was tested by mixing UCNPs with styrene monomer and PS beads. This protocol resulted in polydisperse UCNP-coated PS beads as UCNPs tended to aggregate within the polymers (Fig. 2(b)). In fact, it has been challenging to functionalize UCNPs with polymer coating [32, 33]. We then considered another strategy for coating polymer beads with UCNPs, based on

electrostatic interaction between positively charged UCNPs and oppositely charged polymer beads. Briefly, polystyrene beads with a diameter of  $\sim 2 \mu\text{m}$  were first pre-coated with two polyelectrolyte layers [(PDDA/PSS)] through a facile layer-by-layer assembly approach to provide a uniformly negatively charged surface. Ligand-free UCNPs exhibit positively charged surface. When mixed with negatively charged PS beads, part of the UCNPs suspended in aqueous solution could be attached onto the surface of PS beads due to strong electrostatic attraction. UCNPs coated PS beads were then collected by centrifugation. Due to the ultrasmall size and well-dispersibility, the rest of the ligand-free nanoparticles were left in the supernatant. After centrifugation the nanoparticle supernatant was discarded, and the UCNP-coated PS beads were collected and re-dispersed in an aqueous solution. Then ligand-free UCNPs with positively charged surfaces were absorbed on the surface of PS beads to produce a uniform coating of nanoparticles (Fig. 2(c)).

Fig. 3(a) illustrates the typical process of layer-by-layer assembly and UCNP coating. Bilayers of polyelectrolytes were first deposited onto a PS bead template through alternate adsorption of oppositely charged polyelectrolytes. Next, UCNPs were attached to the bilayer polyelectrolytes due to electrostatic attraction (Fig. 3(b-e)). To create patterned assemblies of UCNP-coated PS beads, photolithography masks with multiple patterns were designed and the photoresist micropatterns were generated by UV photolithography. Fig. 4(a) depicts a schematic procedure for selective assembly of UCNP-coated PS beads. At first, an aqueous dispersion of monodispersed, nanoparticle-coated polystyrene beads was injected into the packing fluidic cell composed of two glass substrates, and the edge of this liquid slug was allowed to move slowly along the meniscus movement direction through a combination of evaporation and capillary flow of the water. The pre-patterned photoresist templates on the bottom substrate could serve as physical traps for retaining the liquid and the polymer beads. As the meniscus front of this liquid slug moves, the capillary force exerted on the polymer beads would be sufficiently strong to drive these beads across the surface of the bottom substrate until they are physically trapped inside the photoresist holes.

When the concentration of PS bead dispersion was high, each template would be filled with a maximum number of the beads, as determined by geometrical confinement. The UCNP-coated PS beads within each hole tended to be in physical contact as a result of

attractive capillary force caused by solvent evaporation (Fig. 4(b-d)). By carefully controlling the size of physical confinement, we were able to realize complex patterns of UCNP-coated PS beads (Fig. 4(e, f)). When compared with previously reported methods, template-directed assembly is particularly attractive because of its high spatial resolution and structural scalability and functional reproducibility.

As a versatile patterning technique, the template-directed assembly allows one to fabricate patterns with different properties and functionalities. Fig. 5(a, b) show the optical and corresponding photoluminescence images of 2D arrays of UCNP-coated PS beads that are formed upon removal of photoresist templates. On the other hand, UCNP-PS composites having different morphologies and optical properties could also be blended to form hybrid functional structures to further construct more complex multicolored barcodes for anti-counterfeiting applications (Fig. 5(c)). One way to increase the compositional and structural complexity of colloidal particles is to sequentially dewet and assemble different types of colloidal particles over the same template substrate. By performing two- or multi-step assemblies of UCNPs/PS composites and choosing different shape hole template, various hybrid aggregates can be formed through this template-assisted assembly process, as shown in Fig. 5(d-h). The photoresist patterns can be easily removed by dissolving with ethanol, and the array of UCNP-coated PS beads could be transferred onto flexible substrates by microcontact stamping.

#### 4. Conclusions

In conclusion, we report the successful experimental demonstration of a high-throughput strategy for large-area, template-directed patterning of UCNPs. We demonstrate the synthesis of UCNP-coated PS beads through a facile layer-by-layer approach. By tailoring the geometry and shape of topological templates through photolithography, multicolor UCNP-coupled PS beads can be selectively patterned on those templates. These results show that capillary force plays a crucial role in directing the self-assembly process. The self-assembled UCNP-coupled PS beads can be used as building blocks to further construct two- and three-dimensional hierarchical structures for nanophotonic applications. We believe that the concept has the potential to pave the way to future design of multifunctional optical devices and sensors.

### Competing financial interests

The authors declare no competing financial interests.

### Acknowledgements

This work is supported by the Singapore Ministry of Education (MOE2017-T2-2-110), Agency for Science, Technology and Research (A\*STAR) (Grant No. A1883c0011), National Research Foundation, Prime Minister's Office, Singapore under its Competitive Research Program (Award No. NRF-CRP15-2015-03) and under the NRF Investigatorship programme (Award No. NRF-NRFI05-2019-0003), and National Natural Science Foundation of China (21771135).

### References

- [1] V. Flauraud, M. Mastrangeli, G.D. Bernasconi, J. Butet, D.T.L. Alexander, E. Shahrabi, et al. Nanoscale topographical control of capillary assembly of nanoparticles, *Nat. Nanotechnol.* 12 (2017) 73.
- [2] N. Liu, M.L. Tang, M. Hentschel, H. Giessen, A.P. Alivisatos, Nanoantenna-enhanced gas sensing in a single tailored nanofocus, *Nat. Mater.* 10 (2011) 631.
- [3] T. Chen, B.M. Reinhard, Assembling color on the nanoscale: multichromatic switchable pixels from plasmonic atoms and molecules, *Adv. Mater.* 28 (2016) 3522.
- [4] YM Wu, M.J.Y. Ang, MZ Sun, BL Huang, XG Liu, Expanding the toolbox for lanthanide-doped upconversion nanocrystals, *J. Phys. D: Appl. Phys.* 52 (2019) 383002.
- [5] X. Qin, JH Xu, YM Wu, XG Liu, Energy-transfer editing in lanthanide-activated upconversion nanocrystals: a toolbox for emerging applications, *ACS Cent. Sci.* 5 (2019) 29.
- [6] H. Dong, L.D. Sun, C.H. Yan, Basic understanding of the lanthanide related upconversion emissions, *Nanoscale* 5 (2013) 5703.
- [7] X. Chen, LM Jin, W. Kong, TY Sun, WF Zhang, XH Liu, et al. Confining energy migration in upconversion nanoparticles towards deep ultraviolet lasing, *Nat. Commun.* 7

- (2016) 1.
- [8] YQ Lu, JB Zhao, R. Zhang, YJ Liu, DM Liu, E.M. Goldys, et al. Tunable lifetime multiplexing using luminescent nanocrystals, *Nat. Photon*; 8 (2014) 32.
- [9] RR Deng, F. Qin, RF Chen, W. Huang, MH Hong, XG Liu, Temporal full-colour tuning through non-steady-state upconversion, *Nat. Nanotechnol.* 10 (2015) 237.
- [10] J. Lee, P.W. Bisso, R.L. Srinivas, J.J. Kim, A.J. Swiston, P.S. Doyle, Universal process-inert encoding architecture for polymer microparticles, *Nat. Mater.* 13 (2014) 524.
- [11] XY Huang, SY Han, W. Huang, XG Liu, Enhancing solar cell efficiency: the search for luminescent materials as spectral converters, *Chem. Soc. Rev.* 42 (2013) 173.
- [12] CL Yan, A. Dadvand, F. Rosei, D.F. Perepichka, Near-IR photoresponse in new up-converting CdSe/NaYF<sub>4</sub>:Yb,Er nanoheterostructures, *J. Am. Chem. Soc.* 132 (2010) 8868.
- [13] P. Rodríguez-Sevilla, Y. Zhang, P. Haro-González, F. Sanz-Rodríguez, F. Jaque, J.G. Solé, et al. Thermal scanning at the cellular level by an optically trapped upconverting fluorescent particle, *Adv. Mater.* 28 (2016) 2421.
- [14] XW Liu, XY Li, X. Qin, XJ Xie, L. Huang, XG Liu, Hedgehog-like upconversion crystals: controlled growth and molecular sensing at single-particle level, *Adv. Mater.* 29 (2017) 1.
- [15] B. Zhou, BY Shi, DY Jin, XG Liu, Controlling upconversion nanocrystals for emerging applications, *Nat. Nanotechnol.* 10 (2015) 924.
- [16] YM Wu, JH Xu, E.T. Poh, LL Liang, HL Liu, J.K.W. Yang, et al. Upconversion superburst with sub-2  $\mu$ s lifetime, *Nat. Nanotechnol.* 14 (2019) 1110.
- [17] ZG Yi, ZC Luo, N.D. Barth, XF Meng, H. Liu, WB Bu, et al. *In vivo* tumor visualization through MRI off-on switching of NaGdF<sub>4</sub>-CaCO<sub>3</sub> nanoconjugates, *Adv. Mater.* 31 (2019) 1901851.
- [18] LL Liang, D.B.L. Teh, N.D. Dinh, WQ Chen, QS Chen, YM Wu, et al. Upconversion amplification through dielectric superlensing modulation, *Nat. Commun.* 10 (2019) 1391.
- [19] K. Zheng, S. Han, X. Zeng, Y. Wu, S. Song, H. Zhang, et al. Rewritable optical memory through high-registry orthogonal upconversion, *Adv. Mater.* 30 (2018) 1801726.
- [20] S. Lamon, YM Wu, QM Zhang, XG Liu, M Gu, Millisecond-timescale, high-efficiency modulation of upconversion luminescence by photochemically derived graphene, *Adv. Opt. Mater.* (2019). 1901345.

- [21] XW Liu, Y. Wang, XY Li, ZG Yi, RR Deng, LL Liang, et al. Binary temporal upconversion codes of Mn<sup>2+</sup>-activated nanoparticles for multilevel anti-counterfeiting, *Nat. Commun.* 8 (2017). 899.
- [22] HL Liu, JH Xu, H. Wang, YJ Liu, QF Ruan, YM Wu, et al. Tunable resonator-upconverted emission (TRUE) color printing and applications in optical security, *Adv. Mater.* 31 (2019) 1807900.
- [23] H.Y. Si, D. Yuan, J.S. Chen, G.M. Chow, H.L. Zhang, Facile patterning of upconversion NaYF<sub>4</sub>:Yb,Er nanoparticles, *J. Colloid Interf. Sci.* 353 (2011) 569.
- [24] MM Jiang, J.A. Kurvits, Y. Lu, A. V. Nurmikko, R. Zia, Reusable inorganic templates for electrostatic self-assembly of individual quantum dots, nanodiamonds, and lanthanide-doped nanoparticles, *Nano Lett.* 15 (2015) 5010.
- [25] N.M. Sangeetha, P. Moutet, D. Lagarde, G. Sallen, B. Urbaszek, X. Marie, et al. Ressler, 3D assembly of upconverting NaYF<sub>4</sub> nanocrystals by AFM nanoxerography: creation of anti-counterfeiting microtags, *Nanoscale* 5 (2013) 9587.
- [26] S. Watanabe, T. Asanuma, H. Hyodo, K. Soga, M. Matsumoto, Calcination-free micromolding in capillaries for nanopatterning of inorganic upconversion luminescent layers on flexible plastic sheets, *J. Colloid Interf. Sci.* 445 (2015) 262.
- [27] S. Watanabe, T. Asanuma, T. Sasahara, H. Hyodo, M. Matsumoto, K. Soga, 3D micromolding of arrayed waveguide gratings on upconversion luminescent layers for flexible transparent displays without mirrors, electrodes, and electric circuits, *Adv. Funct. Mater.* 25 (2015) 4390.
- [28] J.M. Meruga, A. Baride, W. Cross, J.J. Kellar, P.S. May, Red-green-blue printing using luminescence-upconversion inks, *J. Mater. Chem. C* 2 (2014) 2221.
- [29] YH Zhang, LX Zhang, RR Deng, J. Tian, Y. Zong, DY Jin, et al. Multicolor barcoding in a single upconversion crystal, *J. Am. Chem. Soc.* 136 (2014) 4893.
- [30] V. Altoe, D.J. Milliron, B.E. Cohen, P.J. Schuck, S. Wu, D. V. Talapin, et al. Non-blinking and photostable upconverted luminescence from single lanthanide-doped nanocrystals, *Proc. Natl. Acad. Sci.* 106 (2009) 10917.
- [31] D.J. Gargas, E.M. Chan, A.D. Ostrowski, S. Aloni, M.V.P. Altoe, E.S. Barnard, et al. Engineering bright sub-10-nm upconverting nanocrystals for single-molecule imaging, *Nat. Nanotechnol.* 9 (2014) 300.
- [32] J.C. Boyer, N.J.J. Johnson, F.C.J.M. Van Veggel, Upconverting lanthanide-doped NaYF<sub>4</sub>-PMMA polymer composites prepared by in situ polymerization, *Chem. Mater.* 21

(2009) 2010.

[33] NT Deng, XP Zhou, X. Li, XQ Wang, Synthesis of NaYF<sub>4</sub>:Yb,Er/NaYF<sub>4</sub> nanoparticles coated with PAM by *in-situ* polymerization, J. Phys. Chem. Solids. 74 (2013) 480.

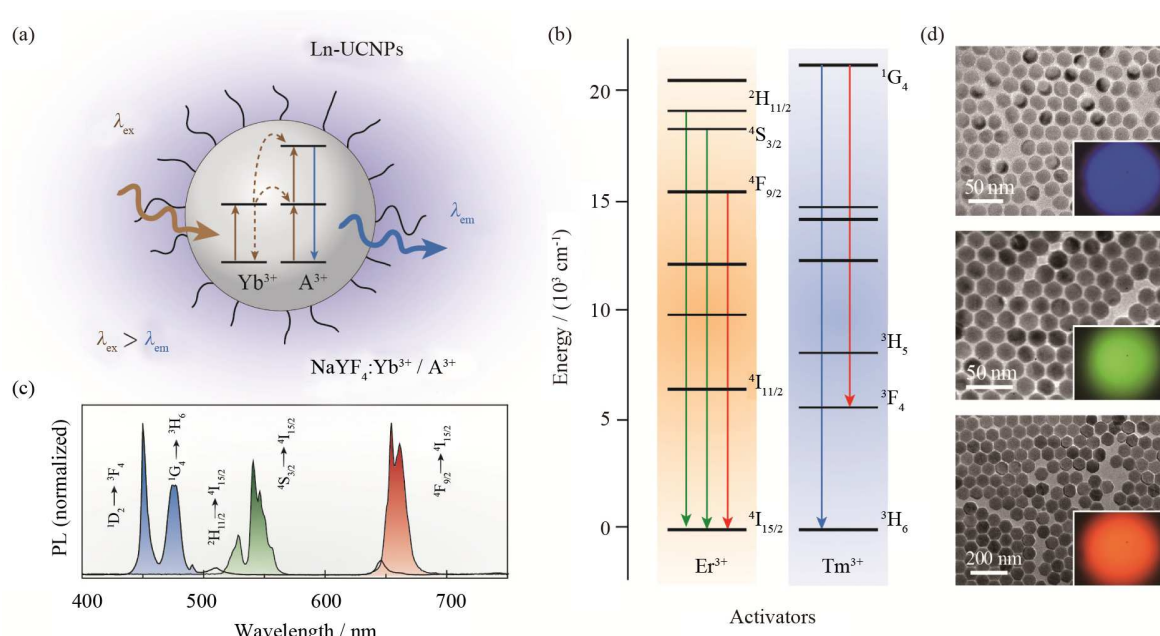


**Fig. 1.** (a) Typical lanthanide-doped upconversion nanoparticles (Ln-UCNPs). NaYF<sub>4</sub> nanoparticles, are co-doped with Yb<sup>3+</sup> sensitizers (red) and activators (blue). NIR excited trivalent yttrium ions can transfer the energy to a nearby activator ion that can generate diverse color emissions from a high energy level; (b) Energy level diagrams of Er<sup>3+</sup> and Tm<sup>3+</sup> activators; (c) Normalized upconversion photoluminescence (PL) spectra of NaYF<sub>4</sub>:Yb/Tm and NaYF<sub>4</sub>:Yb/Er nanoparticles recorded under 980 nm laser excitation; (d) TEM images and the corresponding photoluminescence images (insets) of three types of NaLnF<sub>4</sub> nanocrystals with three primary colours. (top): NaYF<sub>4</sub>:Yb/Tm (30 mol%/0.5 mol%), (middle): NaYF<sub>4</sub>:Yb/Er (5 mol%/2 mol %), and (bottom): NaYF<sub>4</sub>:Yb/Er (60 mol%/2 mol %) nanoparticles.

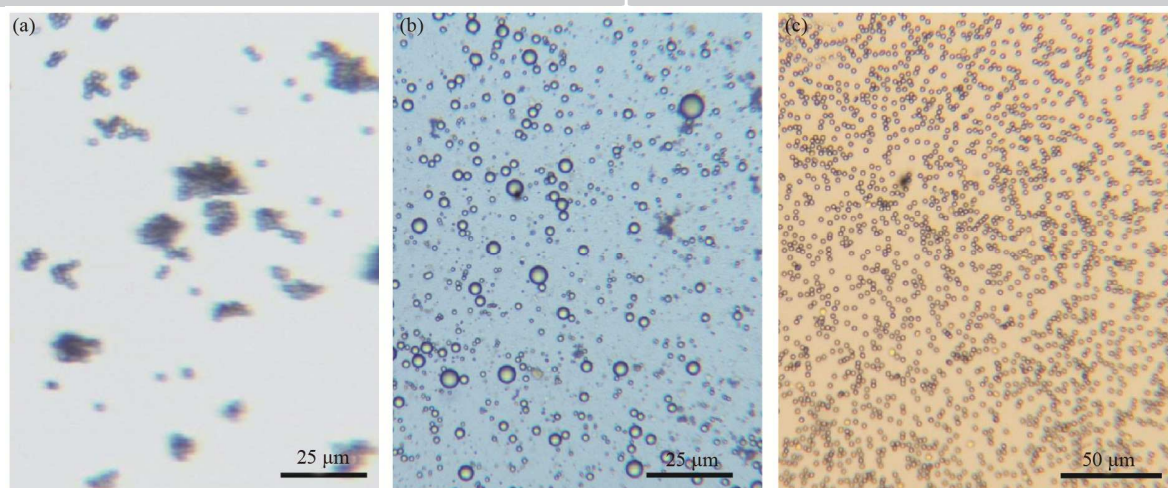


**Fig. 2.** (a) Optical imaging of UCNPs-coated polystyrene beads. This coating, based on a solvent swelling method, results in bead clustering due to strong surface textures; (b) Optical imaging of polydisperse UCNPs-PS bead composites, prepared by an in-situ dispersion polymerization method; (c) Optical imaging of monodisperse and uniform UCNPs-coated PS beads, prepared through layer-by-layer assembly.

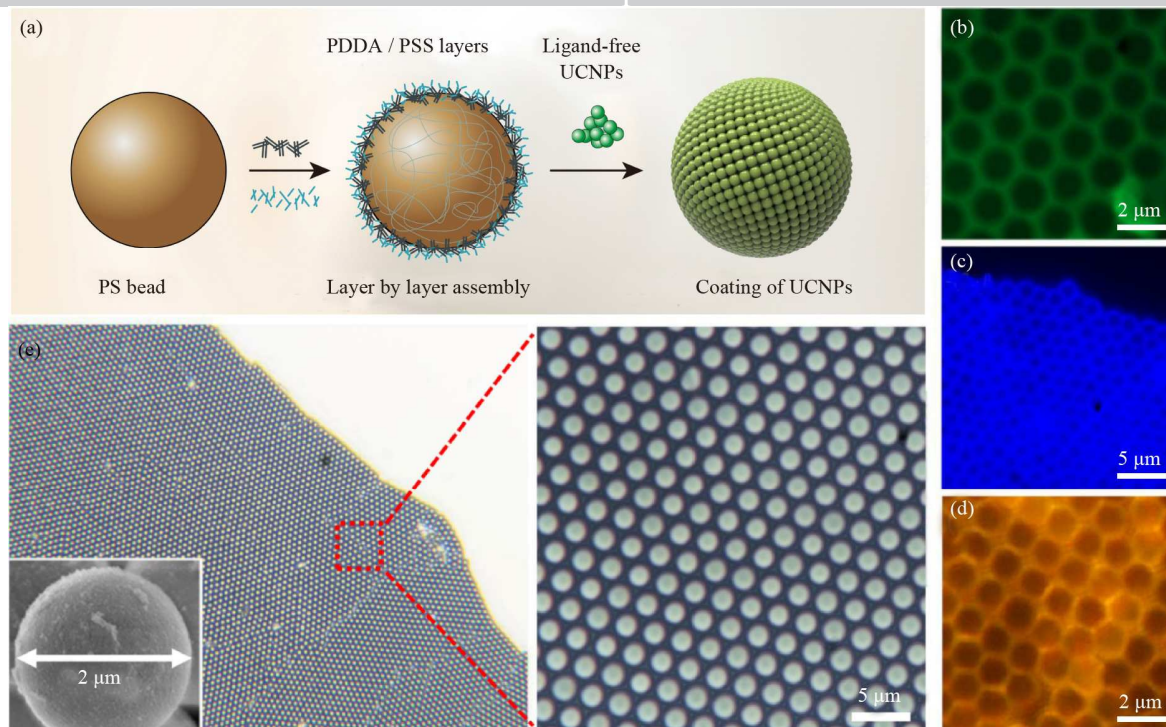


**Fig. 3.** (a) Schematic depicting the protocol of UCNP coating onto PS beads; (b-d) Upconversion photoluminescence images of multicolor UCNP-coated PS beads; (e) Optical microscopy images of typical UCNP-coated PS bead arrays, recorded under white light illumination (Inset: corresponding SEM image of a single UCNP-coated PS bead).

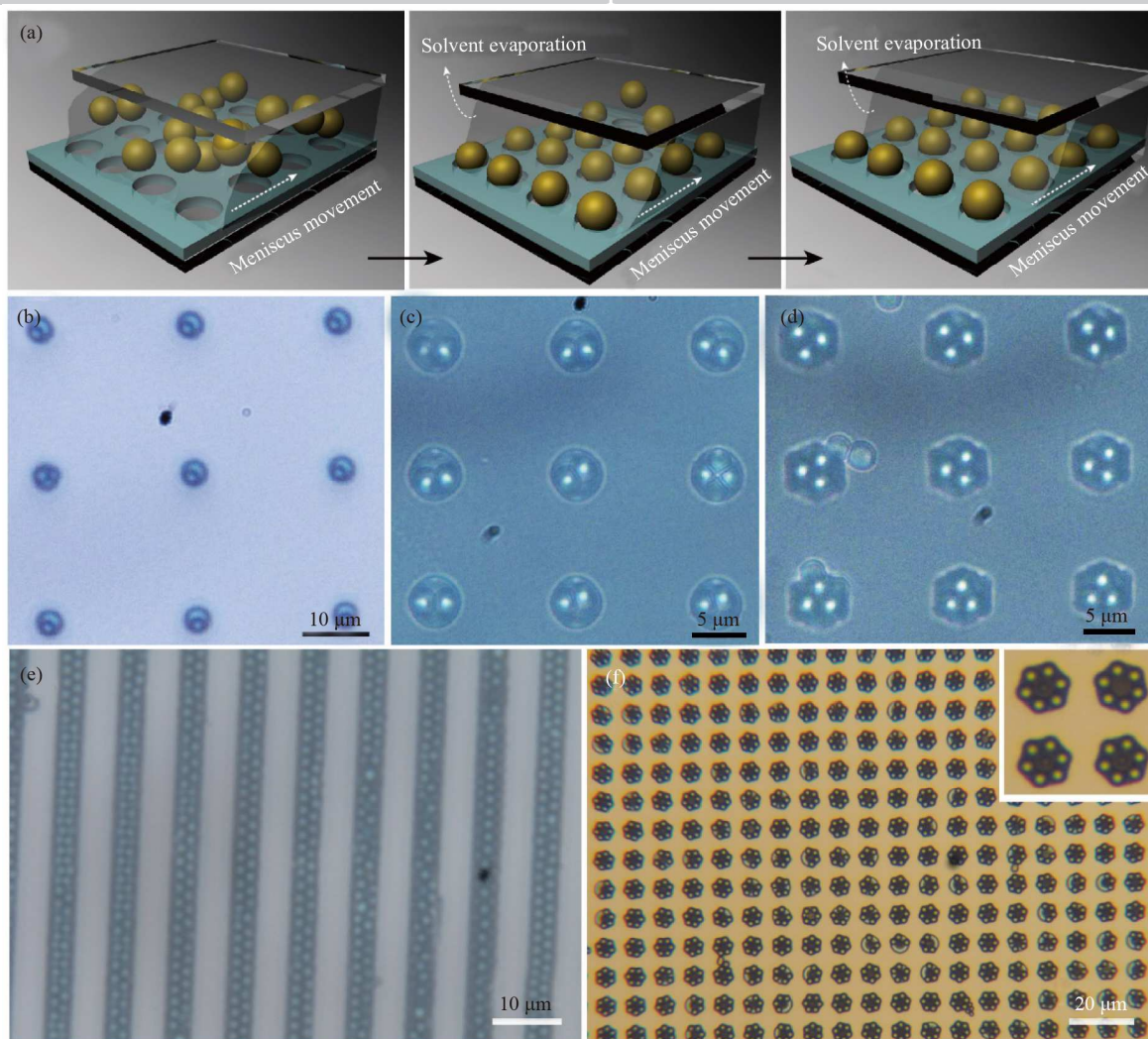


**Fig. 4.** (a) Schematic illustration for site-specific assembly of UCNP-coated PS beads onto a patterned glass substrate. During the assembly process, hydrodynamic flow caused by capillary force within a fluidic cell drives the PS bead assembly on topologically patterned templates; (b-f) Optical images of representative examples of patterned PS beads, showing precise control over the density of the beads at single-bead levels.

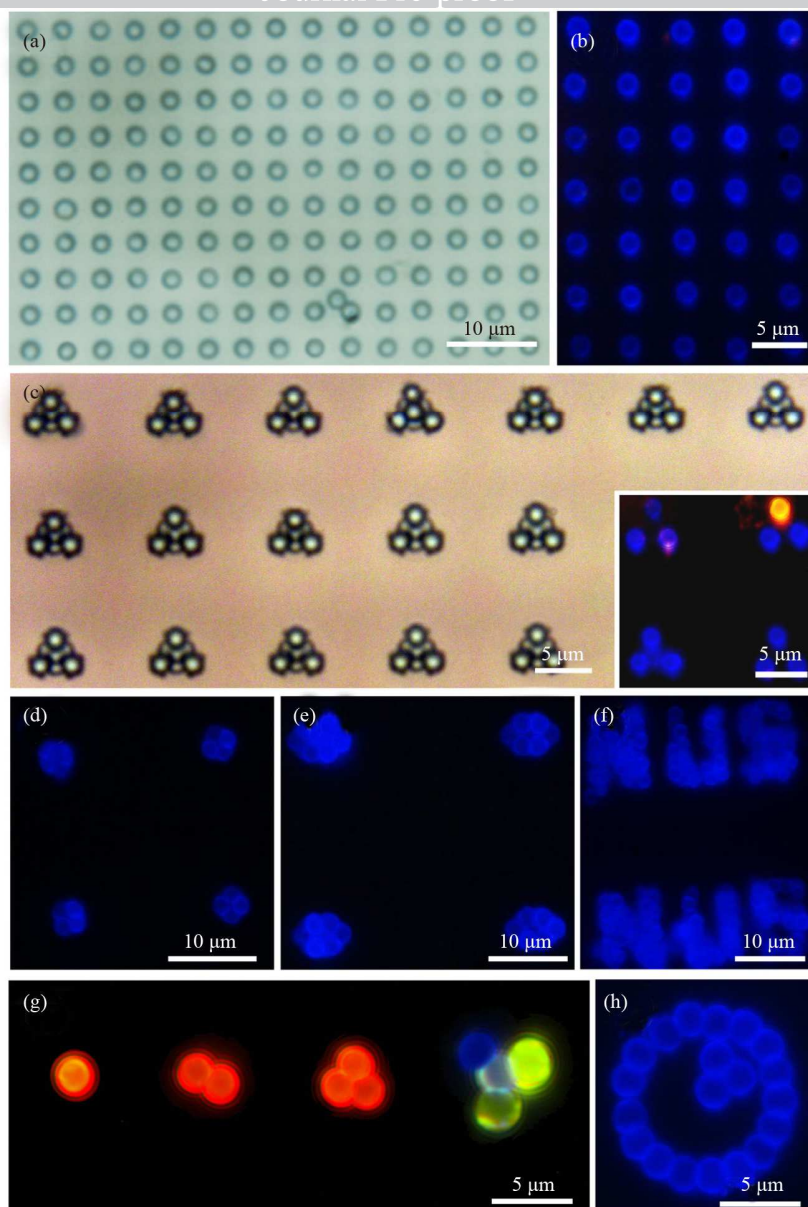
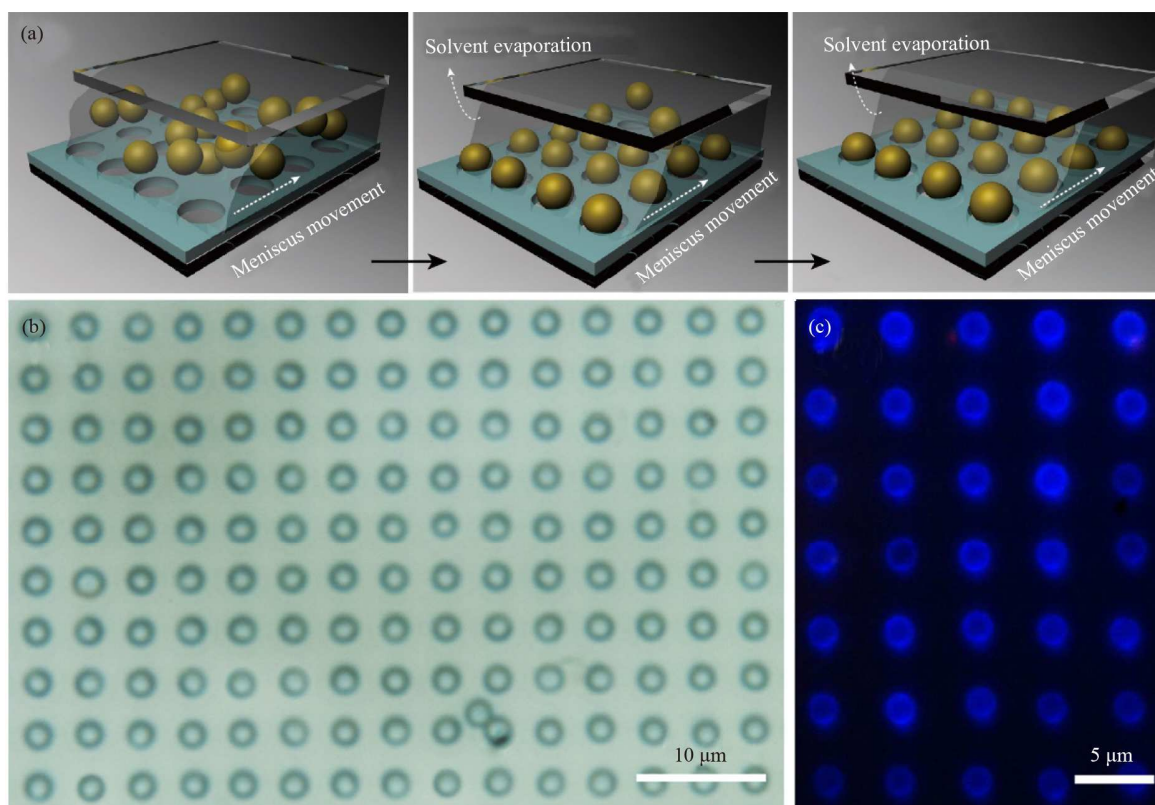


**Fig. 5.** (a-c) Optical microscopy images and corresponding photoluminescence images of singly or triply patterned PS bead arrays; (d-f) Upconversion photoluminescence images of blue UCNP-coated PS bead arrays formed by the template-assisted assembly; (g,h) Upconversion photoluminescence images of multicolor UCNP-coated PS bead arrays formed by the template-assisted assembly.



Lanthanide-doped upconversion nanoparticles (UCNPs) can absorb near-infrared photons and convert them into visible and ultraviolet emissions. These nanomaterials possess extraordinary optical performance and hold potential as active platforms for a variety of technological applications. The ability to fabricate highly ordered nanoparticle-based photonic elements over a large area is of fundamental significance for luminescence tuning. Despite all the efforts made, however, large-area spatial patterning of UCNPs into ordered arrays with high controllability remains a challenge. In this study, we report a high-throughput strategy to pattern optical nanomaterials through the use of polymer microspheres and templated assembly of UCNPs. This technique utilizes capillary force to drive hybrid clusters into the physical template, resulting in large-area, spatially ordered arrays of particles. The findings reported in this work may promote the development of novel nonlinear optical devices, such as solid-state laser arrays, high-density optical storage, and anti-counterfeiting labels.

**Declaration of interests**

The authors declare that they have no known competing financial interests or personal relationships that could have appeared to influence the work reported in this paper.

The authors declare the following financial interests/personal relationships which may be considered as potential competing interests: